Atmopsheric Observance Satellites and Cloud Aerosol Effects

Kiran Sathaye

ABSTRACT

Atmospheric dynamics and indirect effects represent a large portion of the uncertainty in the understanding of Earth's climate systems. One of the most useful tools in analyzing atmospheric processes is the use of satellite data. However, it is known that satellite data can be inaccurate, contributing uncertainty to climate models. To investigate climate change in the Arctic, one of the most vulnerable regions to global climate change, I evaluated the climate over Alaska using satellite-retrieved data. Cloud property changes over the Arctic are useful to understand how surface energy budgets and thus sea ice cover are impacted. To understand changes in clouds over the Arctic, I examined satellite retrievals of aerosol optical depth (AOD), used to indicate pollution levels, and other important climate variables such as liquid effective droplet radius ($R_{eff)}$ for the Alaskan region in the month of April 2008. I analyzed data from three satellite instruments: MODIS, CloudSat, and POLDER. I found that retrievals from MODIS and CloudSat showed greatly differing results for R_{eff} and that MODIS and POLDER showed greatly differing results for cloud cover, with MODIS consistently showing higher values for both parameters. Additionally, no discernible relationship could be found between these two parameters and AOD. These results suggest that the further use of satellite retrievals to analyze the relationship between pollution and cloud properties in the Arctic may prove quite challenging.

KEYWORDS

Aerosol Indirect Effect, Arctic Circle, Climate Modeling, Cloud Properties, Energy Flux

INTRODUCTION

The Earth's atmospheric systems are governed by the presence of many different variables such cloud cover, water content, aerosol content, and temperature, among others. Understanding the complex relationships between these processes is crucial to understanding Earth's climate system and energy budget. The effect of aerosols is of great importance because of their ability to scatter and absorb sunlight, and because of their indirect effect on cloud formation and particle size. These processes all affect atmospheric energy flux, but the exact effects are unknown, contributing to uncertainty in global climate modeling (Cheng et al. 2010). The most effective method for gathering large amounts of atmospheric data on a global scale is satellite remote sensing. Satellites can continuously monitor the globe, making several orbits a day, and therefore quickly produce very large amounts of data.

Figure 1. Map of Region of Interest

Region of interest

The region and time period chosen for this study stretches from 170°W to 140°W and 55°N to 75°N for the month of April 2008. This covers the entire US state of Alaska, and some of the Arctic and Pacific Oceans as well, as shown in figure 1. This region was chosen because of marked warming in the Arctic in recent years, about double the global average (Solomon et al. 2007). Uncertainties in the Arctic climate system stem from complexities in cloud formation and dissipation processes and lack of reliable data (Liu, et al. 2010). Additionally, cloud observance is made increasingly difficult because of the presence of surface snow and ice. The small contrast between the cloud and surface color in the polar regions, combined with low solar flux in the Arctic, makes remote sensing very difficult in this region (Lubin and Morrow 1998). The time period of April 2008 was chosen to coincide with the Department of Energy Indirect and Semi-Direct Aerosol Campaign (ISDAC). The ISDAC study used aircraft-based instruments to measure atmospheric parameters similar to those measured by the satellite systems used in this study. By comparing satellite data from this time period, future studies can compare the aircraft measurements from the ISDAC study to the results of this study to determine satellite accuracy.

Aerosol indirect effect

Aerosols can have many different effects on clouds and solar energy flux. In addition to directly absorbing sunlight, they can act as Cloud Condensation Nuclei (CCN), increasing the number of particles in a cloud and in turn, increasing its reflectivity (IPCC Physical Science Basis, 2007). However, aerosols can also increase the number of ice particles in a cloud, decreasing reflectivity by increasing the amount of transparent ice in the cloud. Because of these varying effects of aerosols in the atmosphere, this study will focus on the effect of aerosols on cloud cover and droplet size, as well as discrepancies between for individual parameters, as measured by different satellite instruments.

Satellite instruments

The first of three satellite instruments used in this study was CloudSat, an atmospheric observance tool launched aboard the NASA satellite CALIPSO (Cloud-Aerosol Lidar and Infrared Pathfinder Satellite Observations) in 2006. This satellite orbits at an altitude of 705 km above the surface in a sun-synchronous orbit, ensuring a constant solar illumination angle. CloudSat uses radar with wavelengths on the order of 1 millimeter, giving greater resolution and detection capability for cloud particle sizes than typical weather radars, which use wavelengths on the order of 1 centimeter. However, this resolution causes CloudSat to record data with a smaller field of view (NASA CloudSat Overview). Because of CloudSat's high resolution and ability to estimate internal cloud conditions, liquid droplet effective radius (R_{eff}) measurements from CloudSat were used in this study.

The second satellite instrument used in this study was the Moderate Resolution Imaging Spectroradiometer (MODIS). This instrument was launched on the satellite Terra, the flagship of the NASA Earth Observing System (EOS) in 1999 and then on Aqua, a satellite launched specifically to monitor global water cycles, in 2002. MODIS uses a broadband radar spectrum to monitor both atmospheric and surface conditions (NASA MODIS Overview). MODIS measurements for cloud cover fraction, aerosol optical depth (AOD), and R_{eff} were used in this study. AOD is a unitless measure of the fraction of light prevented from reaching the surface by aerosol particles over a column of height equal to that of Earth's atmosphere.

The third satellite instrument used in this study was POLDER (POLarization and Directionality of the Earth's Reflectances). Polder was launched on the Parasol satellite in 2004, and is operated by the French Space Agency, CNES. Polder uses a wide-field view radiometer to measure aerosol, atmospheric, and surface conditions on Earth (CNES Polder Overview). The Polder measurements of cloud fraction and AOD were used in this study.

Objectives

The objectives of this study are to determine whether a discernible aerosol effect on cloud cover fraction or R_{eff} can be determined using data from the satellite instruments PODLER, CloudSat, and MODIS. The region and time period to be examined covers the US state of Alaska as well as part of the Arctic Ocean for the month of April 2008. Both inaccurate satellite measurements of these variables as well as lack of coinciding data points are potential hindrances to this goal.

METHODS

Data formats and software

Original satellite data from the three satellites used in this study were created in the Network Common Data Form (NetCDF). NetCDF files are self-describing and can be accessed from any computer architecture. These two features of the NetCDF format make it the preferred choice for satellite data (NASA Data Resources). The data used in this study was converted from the NetCDF format into the RData format, so that statistical analysis could be done using the open source statistical software R (R Development Core Team 2009). Several spatial and temporal corrections and assumptions were made to create a large enough dataset to compare the various atmospheric parameters, which will be further discussed in this section.

Corrections and assumptions

The first correction was made to help create a larger comparable dataset. All variables were averaged over the entire month so that identical points in space and time were not required for comparison. Because these satellite instruments do not generate identical datasets in time and space, taking a mean over the entire time period is the most effective way to create a larger comparable dataset. The satellites cross over the Alaska region 2-4 times per day, and not always in the same location, so the data were averaged over time to be compared spatially. Monthly means were generated using R codes to filter out the datapoints for the specific time period and region of interest. Datapoints were arranged into a 0.1° grid spacing, and values were averaged in the case of more than one existing datapoint for a gridpoint in the time period of interest. These monthly means gave an average value for the entire month for each variable at each point in space. Each dataset was converted into a 300x200 matrix to represent the entire 30° longitude and 20° latitude of the region of interest. To determine the similarity between the R_{eff} measurements taken by CloudSat and MODIS, R was used to determine the summary statistics of each set of measurements, and produce a density plot showing the means and standard deviations of these variables from each satellite. In addition, R was used to create a map image of the datasets, showing increasingly bright colors for high values at each gridpoint over the Alaskan region. The density and summary statistics for the entire region were computed for the cloud cover fraction measurements from MODIS and POLDER as well. In addition to the summary statistics for the entire region, monthly means for 4 sub-regions of with dimensions of 15° longitude and 10° latitude were calculated to determine whether certain regions showed larger discrepancies.

To determine a correlation with AOD, sub-regions of 5°x5° were used and compared with average values for R_{eff} and cloud cover fraction. Only the southernmost sub-regions were used because of sparse Aerosol Optical Depth data created by MODIS, leaving six square regions to analyze. The values for Aerosol Optical Depth were discretized into 4 categories. Optical Depth Ratio values below .1 were designated as “clean” air, values from .1 to .2 were designated as “moderately clean”,.2 to .4 was designated as “moderately polluted”, and above .4 was designated as “polluted”. Values below .06 and above .6 were removed because they likely indicate a different light scattering process or erroneous measurement. R_{eff} and cloud cover fraction means were then computed for each of these 6 regions to determine whether Aerosol AOD and either of these parameters are related. Ice particle size was not used for this detailed analysis because of its high measurement uncertainty.

RESULTS

Datamaps

The measurements for R_{eff} and Cloud Cover Fraction for the entire region proved to have large mean differences as well as large differences in the number of datapoints created. The maps for Cloud Cover Fraction as measured by MODIS and POLDER are seen here, with bright color indicating a higher cloud fraction. These maps show a large difference in resolution, with MODIS showing a datapoint for every possible gridpoint, and POLDER only creating a gridpoint roughly every 0.5°. POLDER roughly shows the outline of the land form of the state of Alaska in its cloud cover region, suggesting higher cloud cover over ocean areas.

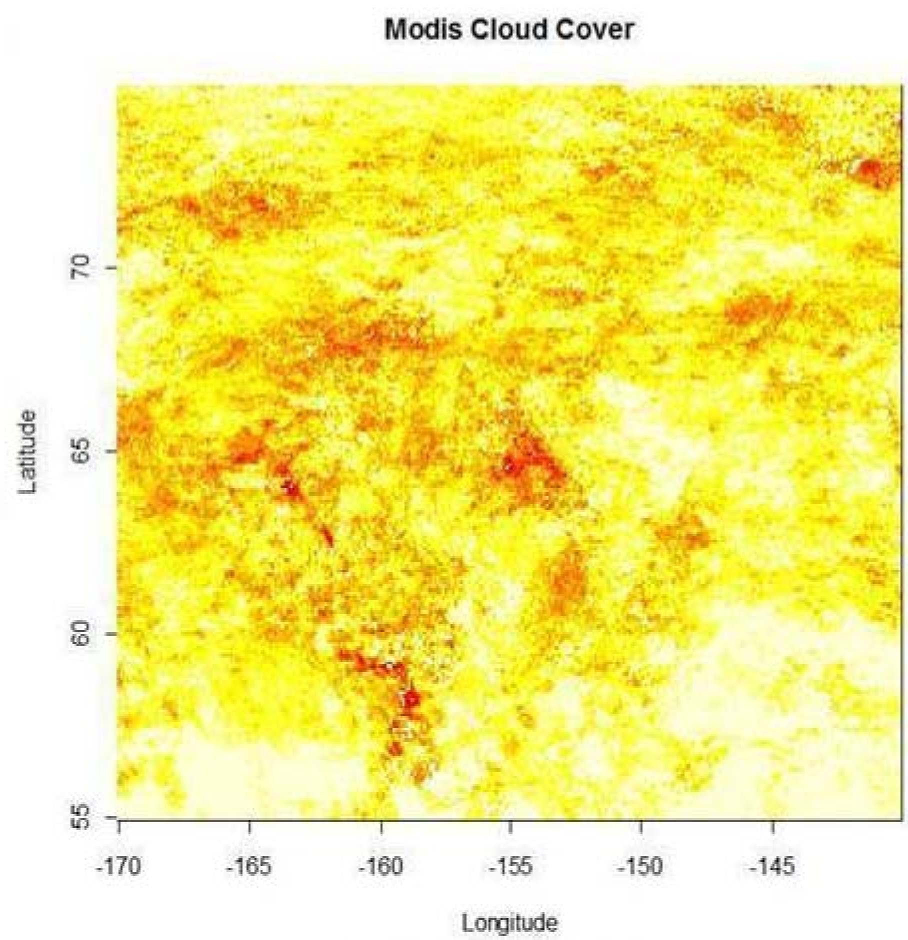

Figure 2. Entire Region MODIS Cloud Cover Map

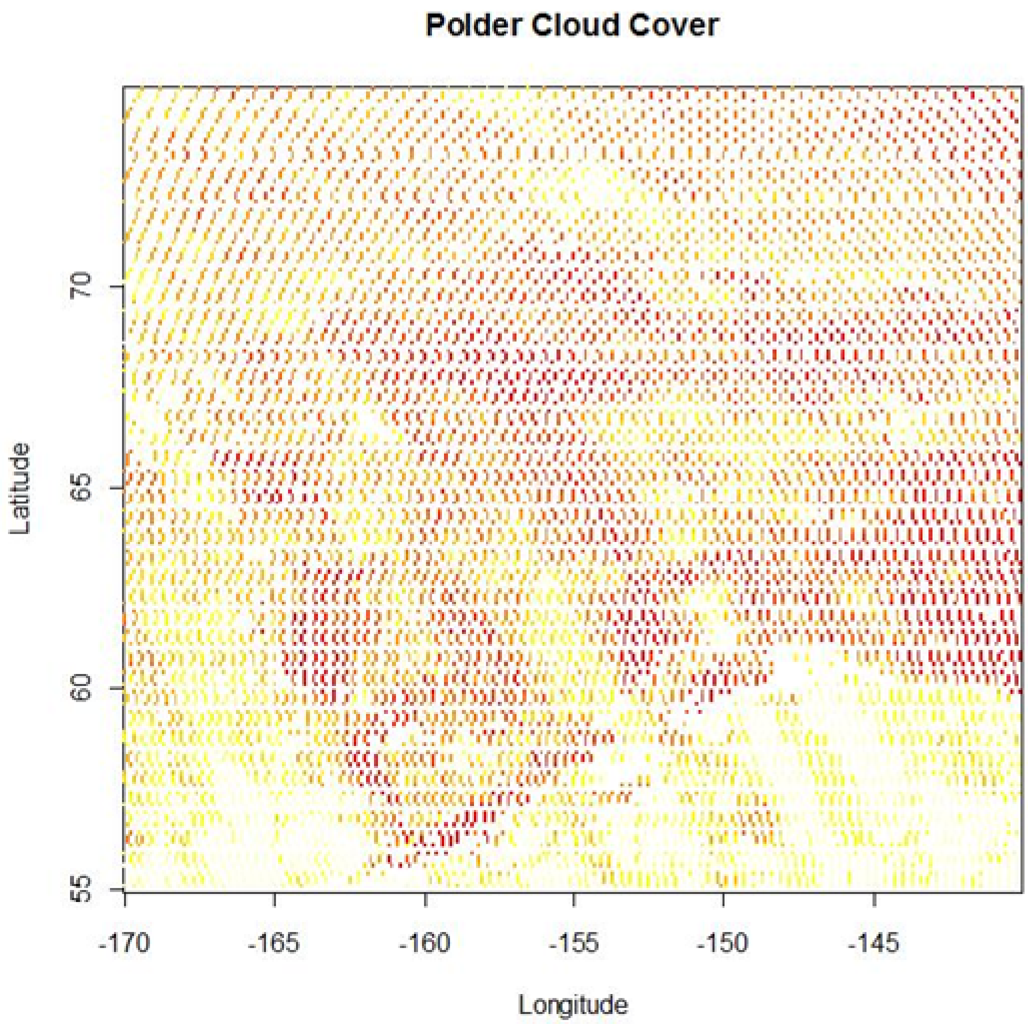

Figure 3. Entire Region Polder Cloud Cover Datamap

R_{eff} maps also showed large differences in the data collected by the satellite instruments. CloudSat uses a narrower field of view, yielding a smaller number of datapoints for each flyover, and creating a clear picture of the orbital path of the satellite. The MODIS map also shows the path of the satellite, but included more datapoints than CloudSat.

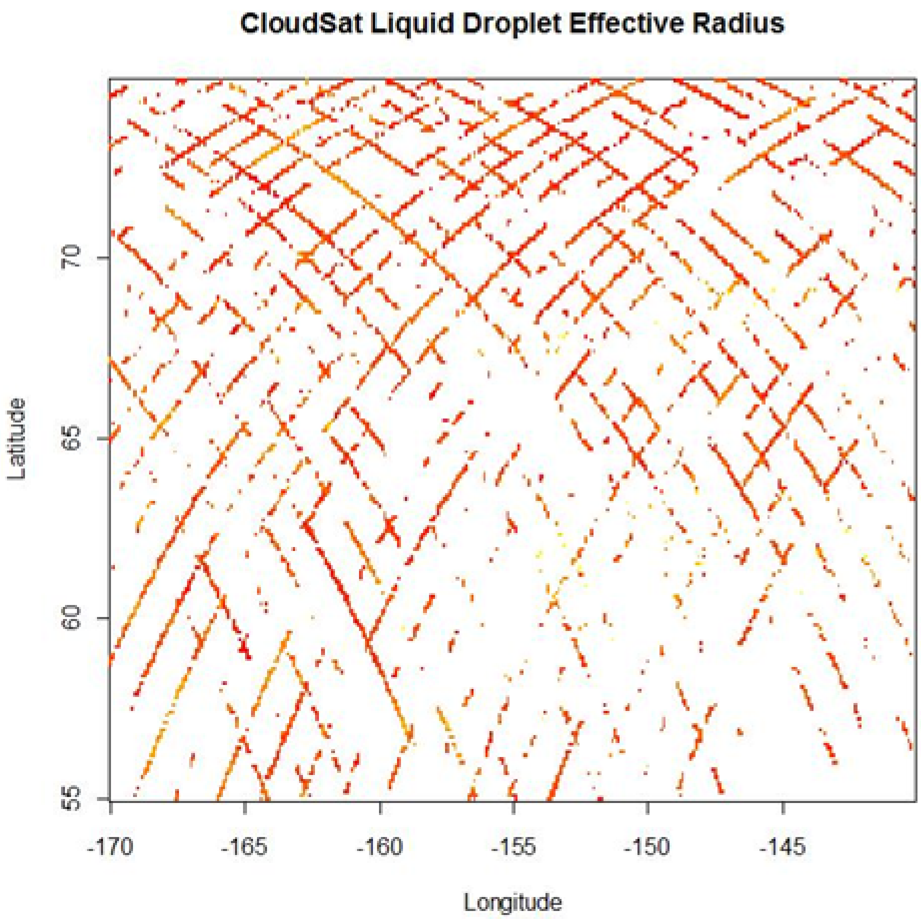

Figure 4. Entire Region CloudSat Droplet Radius Datamap

This datamap clearly shows the satellite path and narrow field of view of CloudSat. There are also many missing datapoints within the satellite's orbital paths, suggesting some calibration or detection issues.

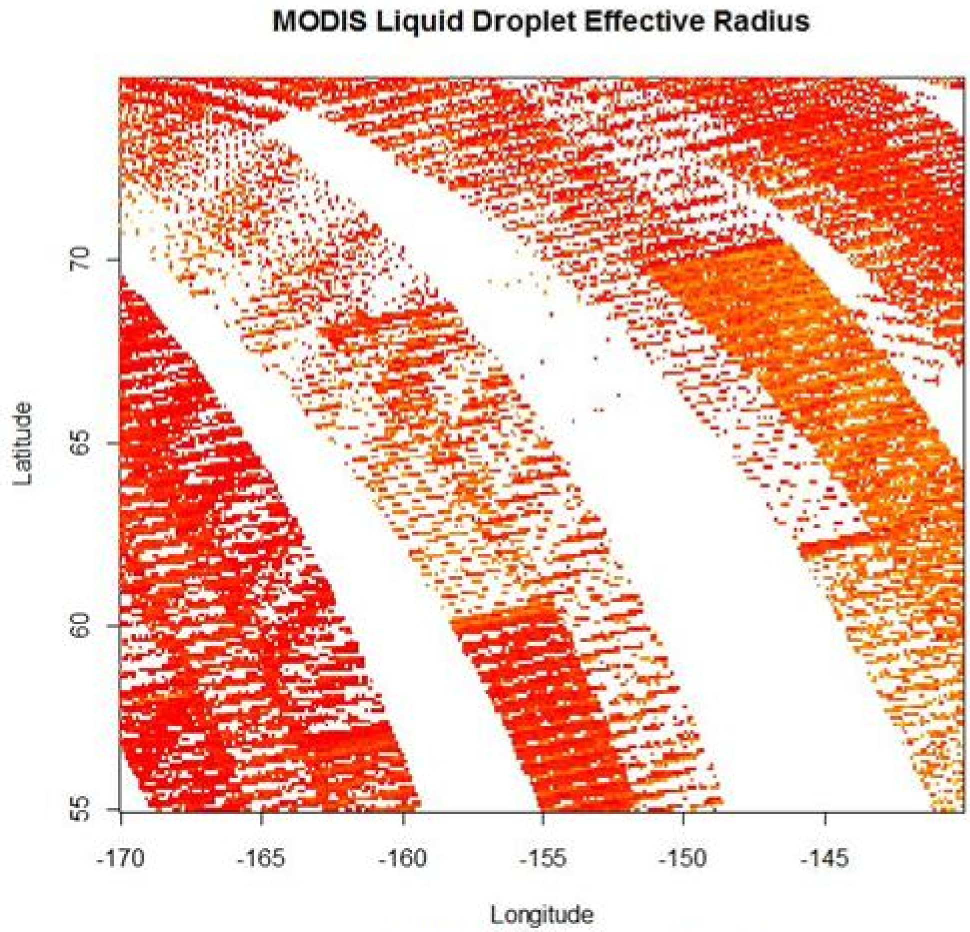

Figure 5. Entire Region MODIS Liquid Droplet Radius Datamap

These maps show that even along the flight path of each of these instruments, some data points are missed by both the narrow and wide view satellite instruments. The four previous maps show the number of Droplet Radius and Cloud Cover Fraction datapoints available for analysis for this region and time period. To determine the overall discrepancy in measurements for these variables, density plots were created to compare the means and distributions of R_{eff} and cloud cover fraction for the entire region, as shown in figures 6 and 7.

Density Plots

The cloud cover fraction measurements for the entire region differ greatly, with the mean fractions differing by 0.252. MODIS reported many more datapoints, as expected from its data map. Both maps show a spike at a fraction value of 1, indicating that there are many instances and locations of complete cloud coverage. Means for smaller sub-regions were also calculated to determine whether one region dominated the discrepancy. Like the cloud cover fraction measurements, the distributions of R_{eff} measurements are very different both in mean and variability, and again MODIS shows a much larger number of datapoints.

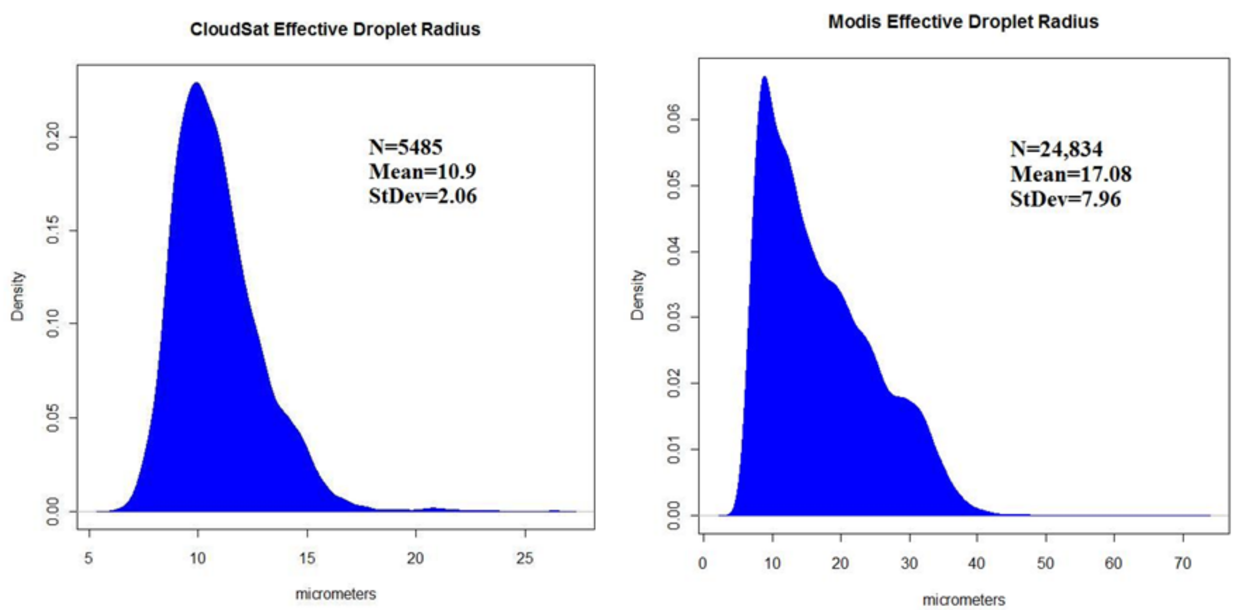

Figure 6. Comparison of Entire Region Liquid Droplet Radius Measurements

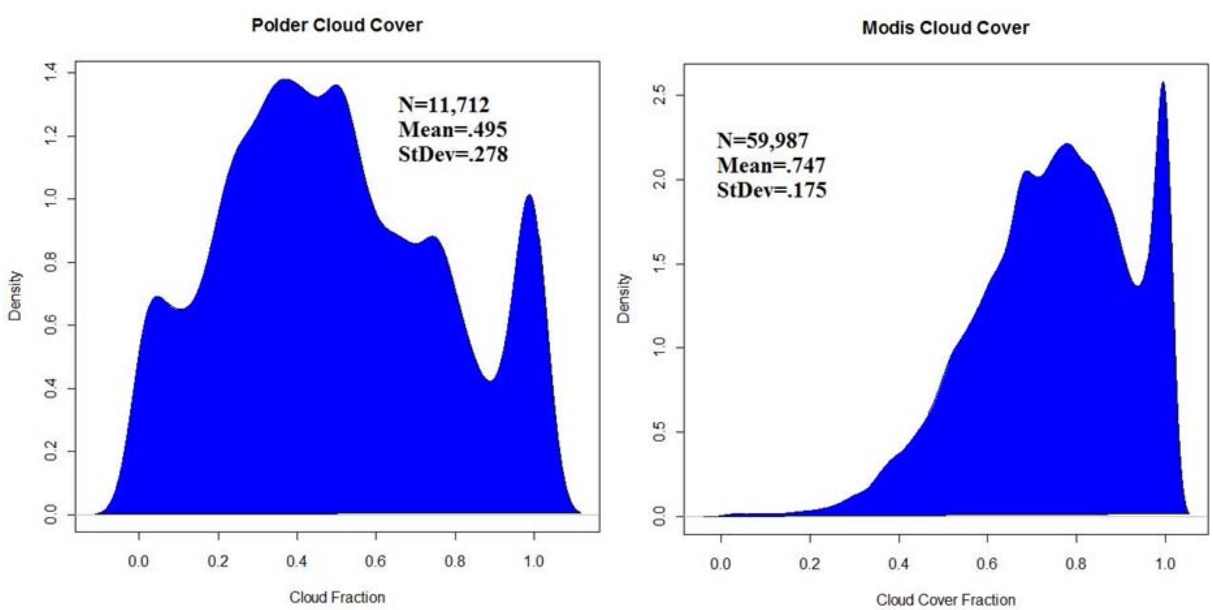

Figure 7. Comparison of Entire Region Cloud Cover Measurments

Analysis of Quadrants

To further detail the discrepancies between R_{eff} and cloud cover fraction measurements, means were calculated for four sub-regions of the Alaskan region. Each sub-region represents a fourth of the area of study. The sub-regions represent the Northwest, Northeast, Southwest, and Southeast quadrants of the overall region of interest. The data in the following table are arranged as such. Table 1 shows the R_{eff} means in micrometers and cloud cover fraction means for each quadrant. The upper-right quadrant represents the means for the Northeast part of the region of interest, the upper-left quadrant represents the Northwest part of the region of interest, and the two lower quadrants represent the two southern quadrants as such. Again, MODIS shows a consistently larger value for droplet size.

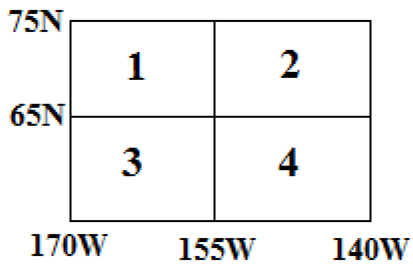

Figure 8. Map of Quadrants

Table 1: Mean Measurements by Quadrant

Instrument and Parameter	Quadrant 1	Quadrant 2	Quadrant 3	Quadrant 4
MODIS Cloud Cover Fraction	0.699	0.726	0.739	0.827
Polder Cloud Cover Fraction	0.405	0.373	0.566	0.53
CloudSat R_{eff} (μm)	10.83	10.616	11.17	11.53
MODIS R_{eff} (μm)	19.77	20.06	18.22	22.26

Aerosol Data

The AOD data obtained from MODIS was used to analyze any possible effect of aerosols on cloud cover fraction and R_{eff}. However, MODIS did not produce a complete AOD dataset for the region, as shown in figure 9. Because the AOD datapoints are concentrated in the southern region, six sub-regions of 5° longitude and 5° latitude were used to analyze potential aerosol effects.

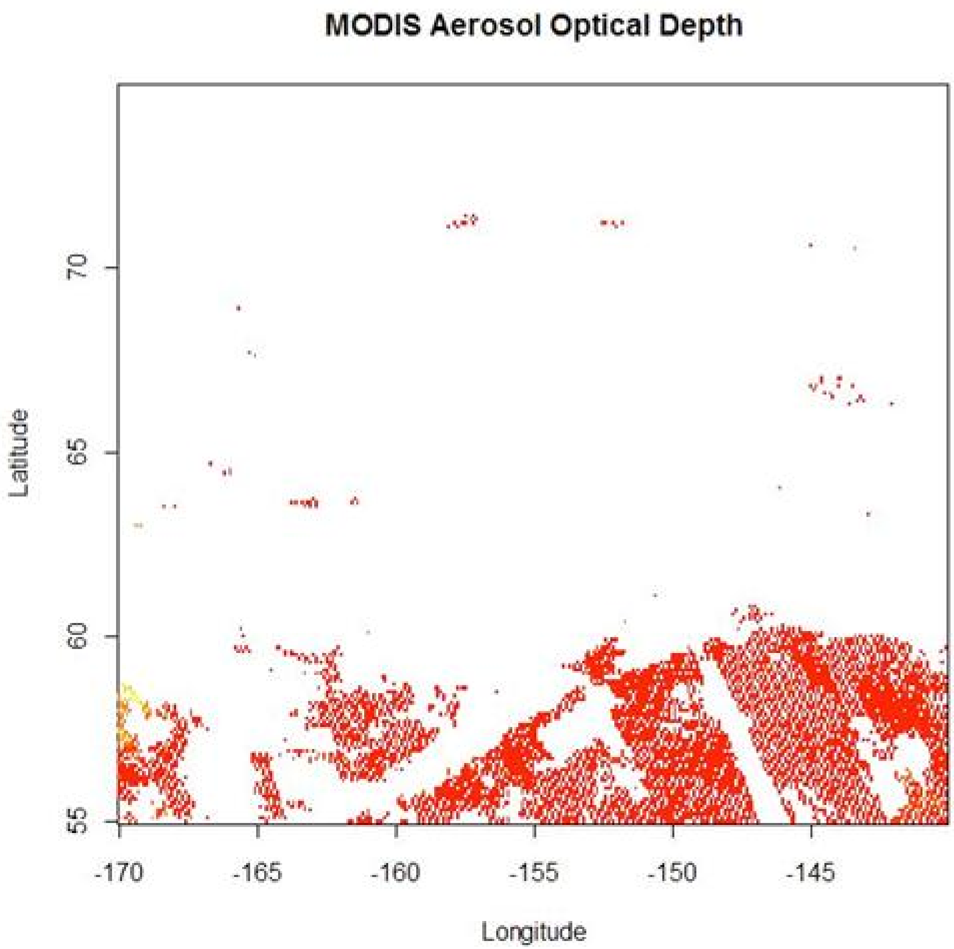

Figure 9. Entire Region AOD Datamap

For the data analysis relating to Aerosol Optical Depth, the southernmost 5° section of the region was broken into six sectors, labeled as such:

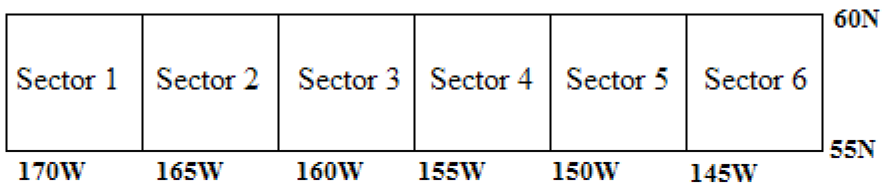

Figure 10. Map of AOD Analysis Sectors

To further simplify the aerosol measurements, the values were discretized into four categories. Table 2 shows the values assigned to each category.

Table 2: Air Quality Categories Based on AOD	
AOD Value	Category
.06-.1	Clean
.1-.2	Moderately Clean
.2-.4	Moderately Polluted
.4-.6	Polluted

For each region, the total number of datapoints in each category was calculated as well as the average value of datapoints in each category. Table 3 shows that most of the Aerosol Optical Depth measurements came in the intermediate categories. The eastern sectors also show higher numbers of measurements, as shown in figure 9. Sector 6 shows the highest percentage of measurements in the Polluted and Moderately Polluted categories, while Sector 4 and Sector 2 show the highest percentage of measurements in the clean air categories.

Table 3: Percentage of Datapoints for Each Category by Sector						
Air Quality Category	Sector 1	Sector 2	Sector 3	Sector 4	Sector 5	Sector 6
Polluted	19.164	5.029	1.642	3.749	1.416	13.16
Moderately Polluted	54.355	43.907	64.696	32.521	53.895	73.532
Moderately Clean	26.132	50.87	33.333	55.483	39.654	13.234
Clean	0	0	0.328	8.247	5.035	0.074
Total Number AOD Points	287	517	609	1067	1271	1345

Table 4: Mean Values Within Each Air Quality Category by Sector						
Air Quality Category	Sector 1	Sector 2	Sector 3	Sector 4	Sector 5	Sector 6
Polluted	0.467	0.49	0.468	0.475	0.431	0.451
Moderately Polluted	0.296	0.265	0.253	0.26	0.294	0.311
Moderately Clean	0.142	0.159	0.17	0.151	0.148	0.171
Clean	NA	NA	0.095	0.08	0.08	0.099
Overall Mean	0.288	0.222	0.228	0.193	0.227	0.311

The average cloud cover fraction and R_{eff} size for each sector was also calculated for comparison with AOD, as seen in Table 5.

Table 5: Cloud Cover and R_{eff} by Sector						
Variable (Mean)	Sector 1	Sector 2	Sector 3	Sector 4	Sector 5	Sector 6
Polder Cloud Fraction	0.796	0.609	0.543	0.712	0.841	0.860
MODIS Cloud Fraction	0.858	0.811	0.767	0.83	0.923	0.936
CloudSat R_{eff} (μm)	11.96	10.99	11.93	11.02	11.00	10.50
MODIS R_{eff} (μm)	17.63	17.67	18.84	18.74	24.27	23.5
Mean AOD	0.288	0.222	0.228	0.193	0.227	0.311

DISCUSSION

The two most meaningful conclusions drawn from the results relate to the accuracy of satellite data and presence of pollutants over the Alaska region. The results shown above plainly indicate a disagreement between MODIS and Polder for cloud cover fraction, as well as between MODIS and CloudSat for R_{eff}. This disagreement further complicates any relationship observed between cloud cover fraction, R_{eff}, and AOD. However, while the means for these variables in the southern sub-region do not obviously indicate any relationships, some interesting conclusions about pollution sources and atmospheric conditions be reached.

Datamaps and resolution

The datamaps in figures 2-5 show greatly varying resolutions and fields of view between the three satellite instruments used in this study. MODIS uses wide-view sensors to create a more complete picture of the atmospheric conditions, while CloudSat only returns data for a relatively narrow band below its orbital path. Polder returned data for the entire region but at a resolution of .5°, compared to the MODIS resolution of .1°. Because of these differences in resolution and number of datapoints, using spatial and temporal means to compare the data returned by these may cause some details in the information to be lost. Means over a certain region in space and time may not accurately represent the same atmospheric conditions.

Aerosol correlations and global comparisons

The density plots for R_{eff} and cloud cover fraction show very large differences between satellite measurements. The MODIS mean R_{eff} measurement of 17.08 µm is much higher than the CloudSat measurement of 10.9 µm. MODIS is known to overestimate many measurements, and the CloudSat high resolution and narrow field of view likely make it a more accurate instrument for this parameter (Kaufman et al., 2005). The overall means for cloud cover fraction showed a similar disparity, with MODIS returning a mean of 0.747 and POLDER returning an overall mean of 0.495. The correct value is more difficult to determine in this case because of the difference in resolutions, but it can be seen in figures 2 and 3 that both instruments show increased cloud cover over sea, and more specifically in the southeast and southwest corners of the region of interest.

This study also attempts to show atmospheric indirect effects due to heightened aerosol presence. As shown in figure 9, AOD data was only available in the southernmost 5° of the region of interest. Therefore, the data in this region was split into 6 sectors, showing longitudinal differences in AOD and the parameters it was expected to influence. The following figure shows global average values for MODIS AOD measurements, and provides some explanation for the longitudinal AOD differences seen in table 4.

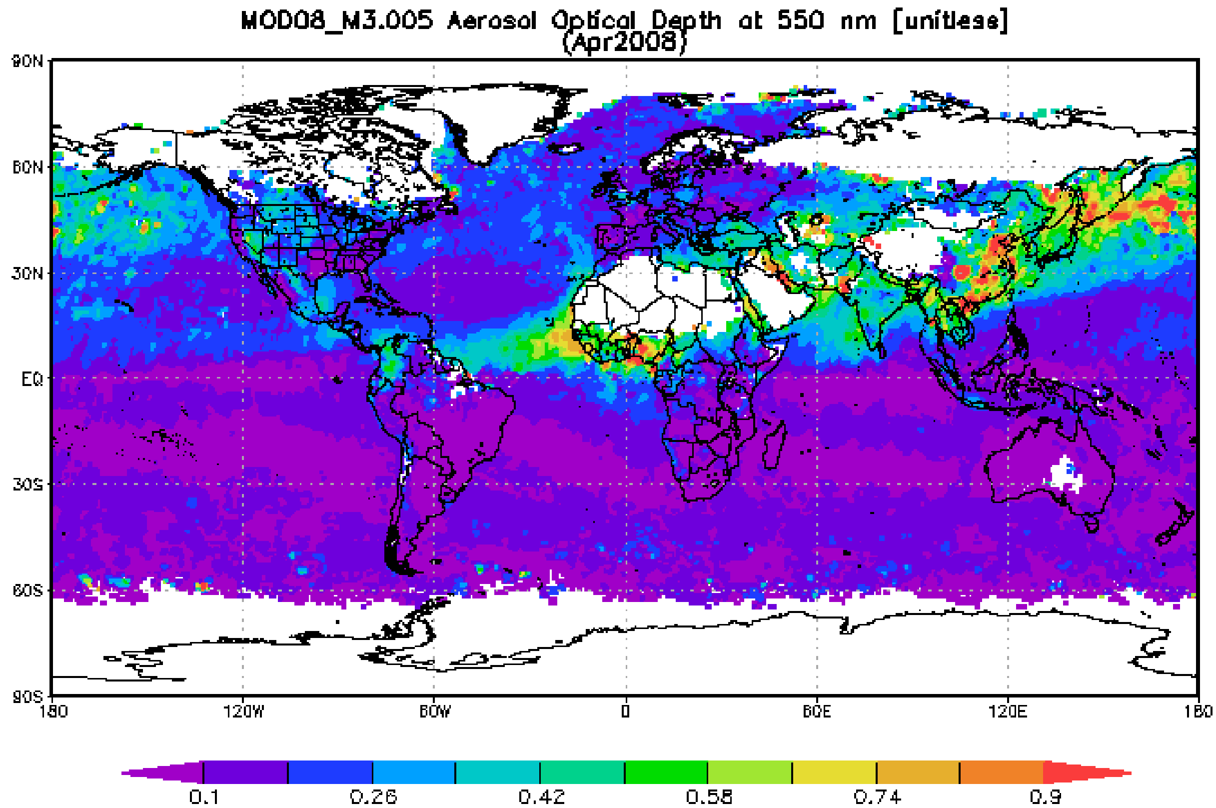

Figure 11. Global Mean MODIS AOD Measurements for April 2008

Courtesy: NASA

This figure shows some interesting trends for various parts of the globe. For example, the aerosol plume stretching from West Africa into the Atlantic is caused by forest fires, prevalent in this region during April (Korontzi, 2005), and ocean regions are shown to have much cleaner air because they are far removed from pollution sources on land. MODIS does not have many data points for both the Antarctic and Arctic regions, which explains the lack of northern datapoints in figure 9. In table 4, it can be seen that the two most polluted sectors are sectors 1 and 6. These sectors represent the extreme southwest and southeast corners of the region of interest. From this figure, it can be seen that this increased pollution is likely caused by aerosols from East Asia in sector 1 and aerosols from the western United States in sector 6. Additionally, the sector 1 AOD mean value of .288 may be an underestimate due to its low number of datapoints. Sector 1 returned only 287 datapoints while sector 6 returned 1345 datapoints with a mean AOD of .311 as shown in tables 3 and 4.

One of the indirect effects of aerosols in the atmosphere is a reduction in mean R_{eff}, with an increase in aerosol concentration for a cloud with fixed water content reducing the effective size of the droplets formed (Feng and Ramanthan 2010). The global R_{eff} means for April 2008 show this trend in many of the locations with high aerosol content as shown in figure 11.

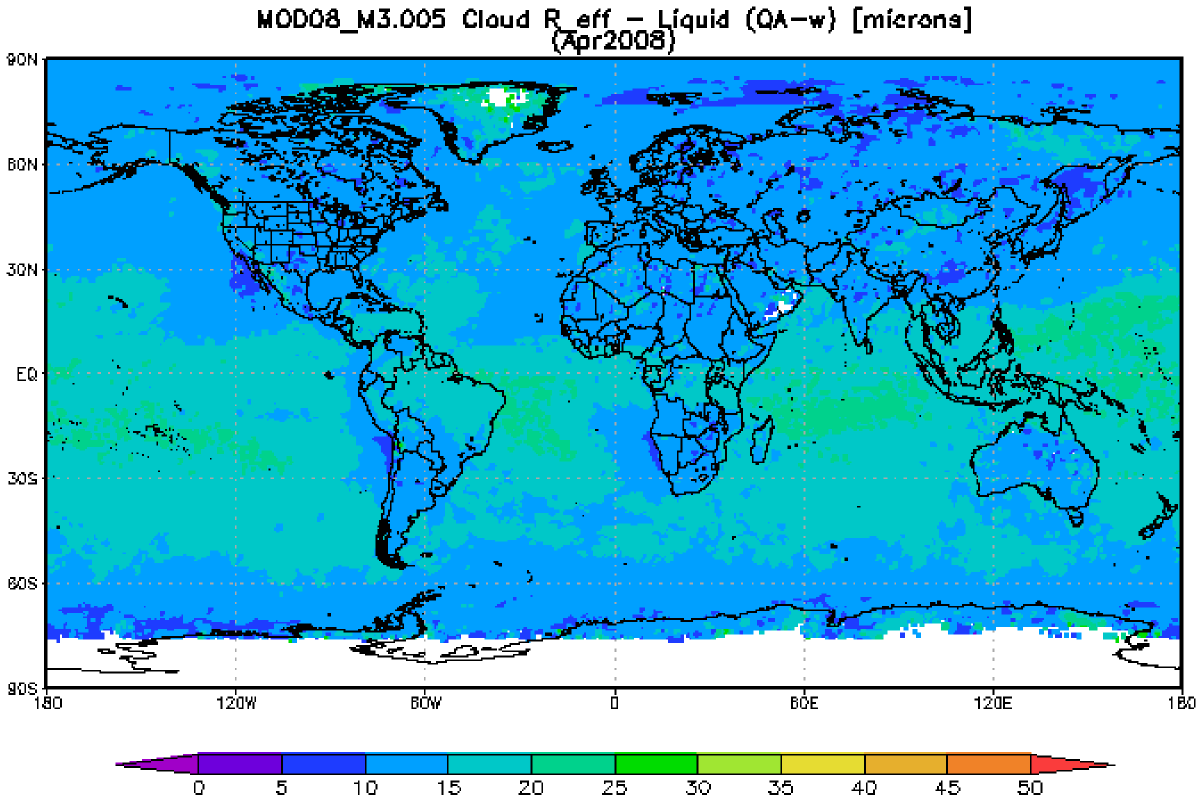

Figure 12. Global Mean MODIS Droplet Effective Radius Measurements for April 2008
Courtesy: NASA

A notable decrease in R_{eff} can be seen in East Asia, off the western United States, and above the Arctic Sea, a region that MODIS does not return AOD data. Ocean regions show the highest R_{eff} values, corresponding to the low aerosol concentrations due to separation from combustion sources. All of the sectors listed in table show R_{eff} values between 9 and 25 microns. These approximate values are also seen in figure 12. However, the correlation with AOD is not clearly seen in table 4 for the sectors chosen. CloudSat data showed sector 6 to have the lowest R_{eff}, which is expected because this sector had the highest mean AOD. However, MODIS showed a high mean for this sector, 23.5 microns. Not only do both satellites differ greatly on the actual values of mean R_{eff} for each sector, but they are in disagreement as to which sector has the smallest and largest R_{eff}. Only sector 5 had a higher mean R_{eff} measured by MODIS. Additionally, CloudSat reported its highest mean R_{eff} in sector 1, which was determined to be the 2nd most polluted sector by the MODIS AOD data. In contrast, MODIS reported sector 1 to have the lowest mean R_{eff} of all the sectors, which would seem to correlate with the MODIS AOD data. These differences can be attributed to a low importance of aerosols on R_{eff}, or to poor satellite data retrievals for AOD. Neither set of satellite measurements for R_{eff} shows the expected inverse correlation with AOD for all sectors, and in fact the two R_{eff} datasets do not agree on overall mean R_{eff} or mean R_{eff} for each sector. These discrepancies suggest that the lack of observed correlation with AOD can be at least partially attributed to inaccurate satellite data.

The global map for Cloud Cover Fraction is not included because many other factors have a greater influence on cloud presence than AOD on a global scale. With increased AOD and smaller R_{eff}, cloud droplets do not grow large enough to precipitate, increasing cloud cover fraction. Clouds are also influenced by many other meteorological factors, which makes discerning the aerosol indirect effect more challenging (Menon et al. 2008). However, many important conclusions can be drawn from the Cloud Cover Fraction data examined in this study. Figure 7 and Table 1 both show a large discrepancy in the mean measurements for Cloud Cover Fraction made by MODIS and POLDER. The MODIS mean was 50% higher than the mean measured by POLDER. For the quadrant sub-regions, both instruments identified the southern quadrants as having the highest cloud cover. Previous studies show a correlation between increased Cloud Cover Fraction and AOD (Kaufman et al., 2005b), which can be seen for some of the means in Table 5.

When Cloud Cover Fraction was examined by sector for the southernmost 5°, the far eastern and western sectors were identified as the highest cloud cover fraction sectors. This seems to agree with the data for AOD. However, these higher values may be due to the low presence of land in these sectors. The Aleutian island arc cuts through sectors 2 and 3, as seen in figure 1, and figure 3 shows a rough land outline relating to Cloud Cover Fraction. These sectors also show the lowest mean Cloud Cover Fraction measured by both POLDER and MODIS. Ocean regions usually have higher cloud cover, and raised landforms can act to break up cloud formations, possibly causing the lower Cloud Cover Fractions in the interior sectors.

CONCLUSION

Accurate collection of atmospheric data is extremely important to understanding the processes that govern atmospheric dynamics and energy fluxes in the Arctic region. Existing satellite instruments differ greatly in their measurements of atmospheric variables such as R_{eff} and Cloud Cover Fraction. An additional hindrance to the understanding of atmospheric processes is an incomplete understanding of the effect of aerosols on other atmospheric parameters. The dataset examined in this study for Arctic AOD is incomplete due to difficulty obtaining complete satellite retrievals for AOD over the Arctic Circle. Although some correlation was seen in this study between AOD, cloud cover fraction, and R_{eff}, the data examined did not prove to be definitive enough to further quantify any relationships between aerosols and cloud properties. In some cases, data from two different satellites indicated that different regions contained the highest R_{eff} and cloud cover fraction, further obscuring any potential relationship. Better methods for aerosol detection in polar regions and greater agreement between satellites measuring atmospheric parameters could help further illuminate and quantify Arctic atmospheric processes.

ACKNOWLEDGEMENTS

I would like to thank my mentor Surabi Menon, as well as everyone at LBNL EETD that helped me with this project, and my ES 196 instructors and classmates for review and help throughout the writing process.

REFERENCES

Cheng, T.H., Gu, X.F., Yu, T., Tian, G.L., The reflection and polarization properties of non-spherical aerosol particles. Journal of Quantitative Spectroscopy and Radiative Transfer. 111: 895-906.

CNES Polder Overview. 2010 < http://smsc.cnes.fr/POLDER/>

Feng, Y and Ramanthan, V. 2010. Investigation of aerosol–cloud interactions using a chemical transport model constrained by satellite observations. Tellus. 62.1.69-86.

Intergovernmental Panel on Climate Change (2007), Climate Change 2007: The Physical Science Basis, edited by S. Solomon et al., Cambridge Univ. Press, New York.

Kaufman, Y., I. Koren, L. Remer, D. Rosenfeld, and Y. Rudich. 2005a

The effect of smoke, dust, and pollution aerosol on shallow cloud development over the Atlantic Ocean, Proceedings of National Academy of Science.32, 11,207–11,212.

Kaufman, Y. J., I. Koren, L. A. Remer, D. Tanre´, P. Ginoux, and S. Fan 2005b. Dust transport and deposition observed from the Terra-Moderate Resolution Imaging Spectroradiometer

(MODIS) spacecraft over the Atlantic Ocean, Journal of Geophysical Research.110, D10S12, doi:10.1029/2003JD004436

Korontzi, S. 2005. Seasonal patterns in biomass burning emissions from southern African vegetation fires for the year 2000. Global Change Biology. 11.10.1680-1700

Liu, Y., Ackerman, S., Maddux, B., Key, J., Frey R. 2010. Errors in Cloud Detection over the Arctic Using a Satellite Imager and Implications for Observing Feedback Mechanisms. American Meteorological Society Journal of Climate. 23: 1894-1907

Lubin, D. and E. Morrow, 1998. Evaluation of an AVHRR cloud detection and classification method over the central Arctic Ocean. Journal of Applied Meteorology. 37:166–183.

Menon, S., Del Genio, A., Kaufman, Y., Bennartz, R., Koch, D., Loeb., Orlikowski, D. 2008. Analyzing signatures of aerosol-cloud interactions from satellite retrievals and the GISS GCM to constra in the aerosol indirect effect. Journal of Geophysical Research 113. D14S22, doi:10.1029/2007 JD009442

NASA CloudSat Overview. 2010. <http://www.nasa.gov/mission_pages/cloudsat/mission/index.html>

NASA Earth System Science Data Resources. 2005.

NASA MODIS Overview. 2010 < http://modis.gsfc.nasa.gov/>

R Development Core Team (2009). R: A language and environment for statistical computing. R Foundation for Statistical Computing, Vienna, Austria. ISBN 3-900051-07-0, URL http://www.R-project.org.

Solomon, S., D. Qin, M. Manning, Z. Chen, M. Marquis, K. B. Averyt, M. Tignor, and H. L. Miller, 2007. Summary for policymakers. *Climate Change 2007: The Physical Science Basis*, S. Solomon et al., Eds., Cambridge University Press, 1–18.